Supplementary Figure S1

NH Staunstrup et al. 2017

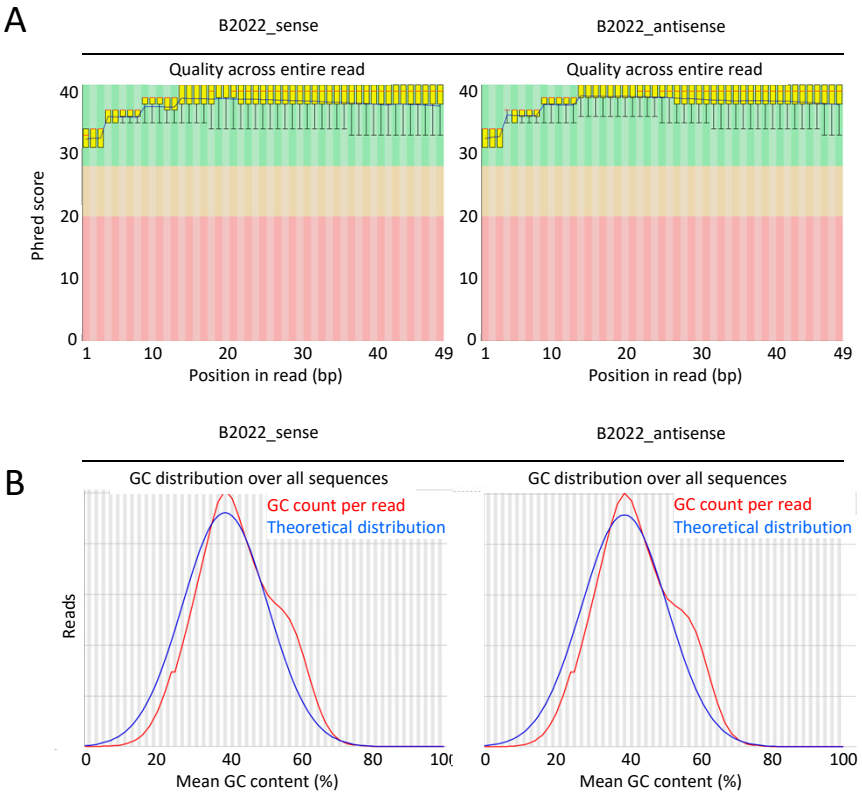

Supplementary Figure S1: Representative FastQC outputs. Quality of sequence data exemplified by the output of the B2022 sense and antisense sequencing reactions. (**A**) Sequencing quality (Phred) score across the PE50 reads; (**B**) GC content in the MeDIP enriched samples (red line) compared to the theoretical distribution (blue line).

Supplementary Figure S2

NH Staunstrup et al. 2017

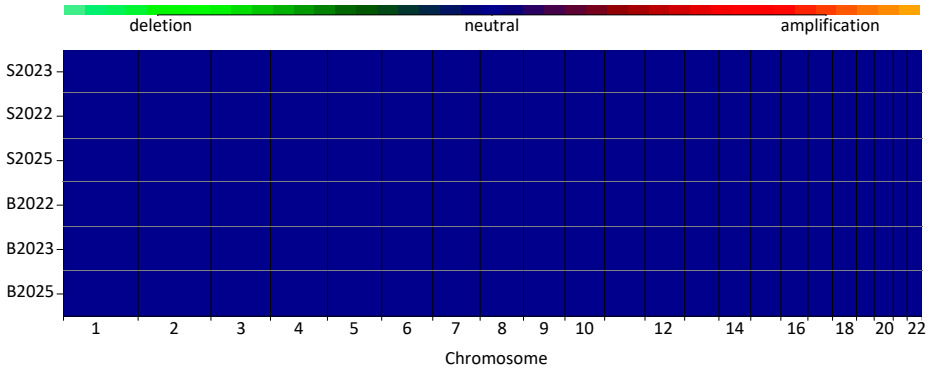

Supplementary Figure S2: CNV analysis for existence of chromosomal copy number abnormalities in the blood and saliva samples. Based on the HMMcopy R package and ≥1 Mb genomic windows.

Supplementary Figure S3

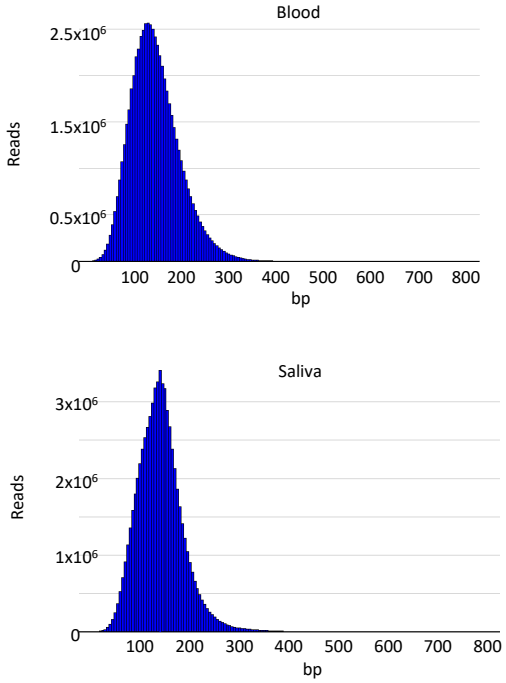

Supplementary Figure S3: Normal distribution of sequencing read length. Length distribution of all filtered and mapped reads in the grouped saliva and blood sample sets.

Supplementary Figure S4

NH Staunstrup et al. 2017

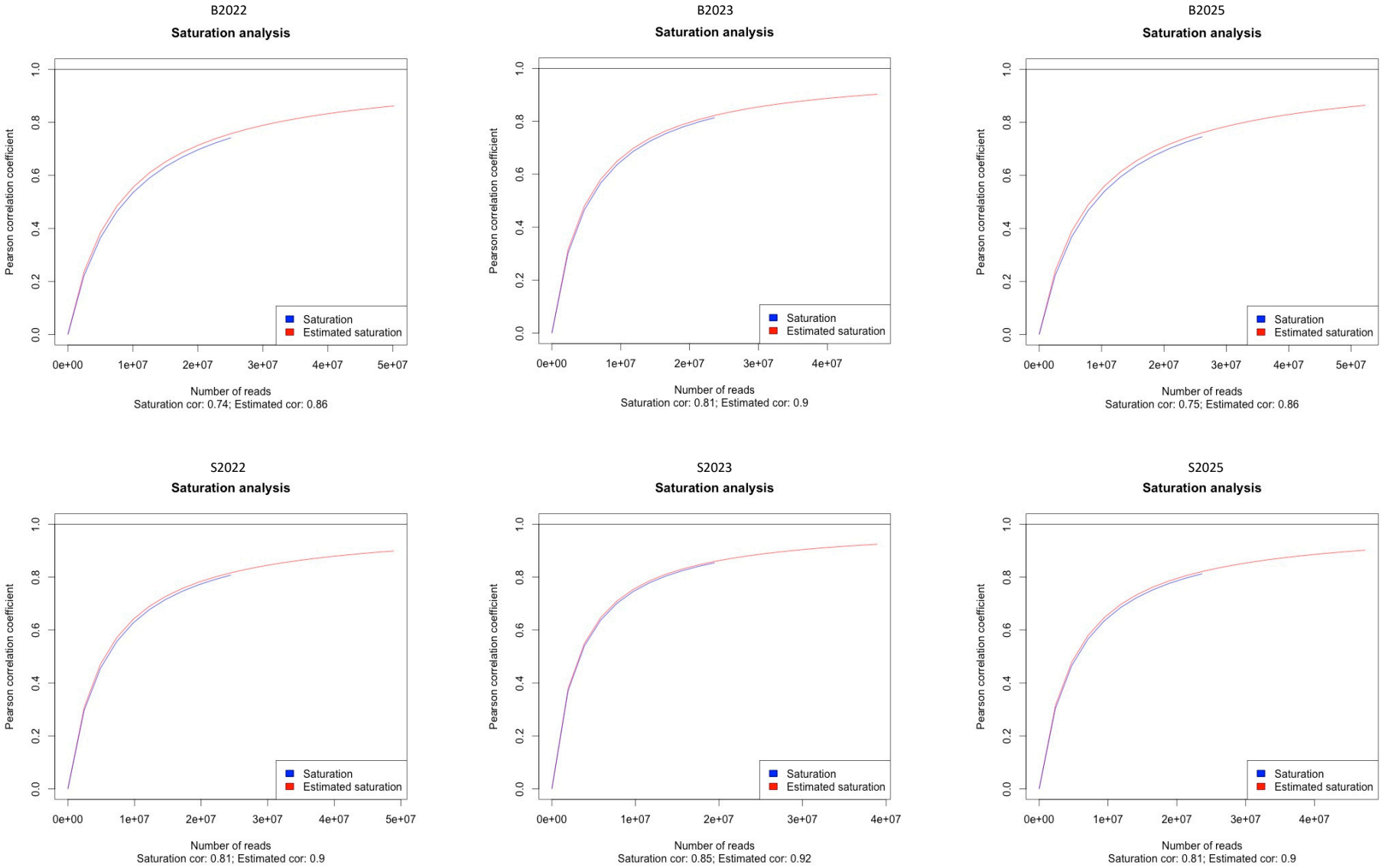

Supplementary Figure S4: Saturation plots depicting comparable complexity and depth among all samples. Saturation plot showing adequate complexity and reproducibility of mapped reads in the six samples compared to the reference genome.

Supplementary Figure S5

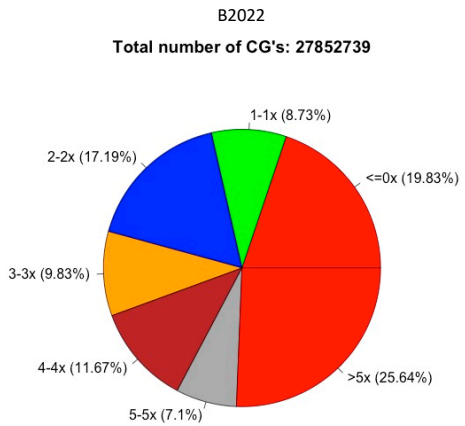

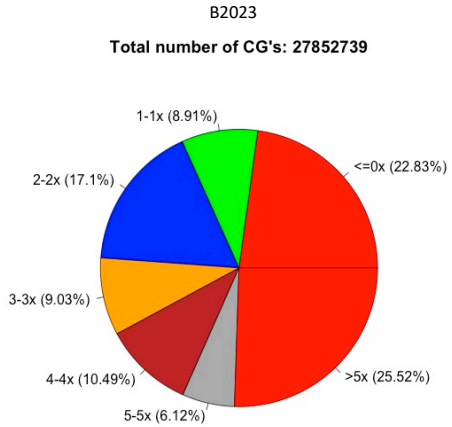

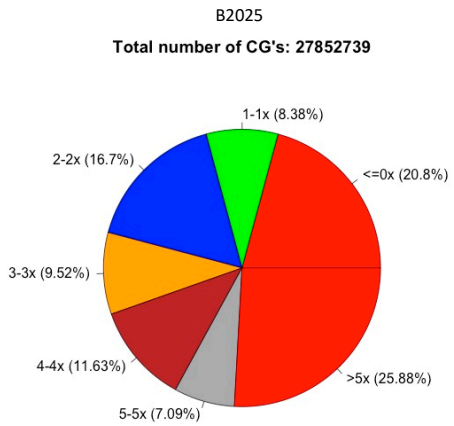

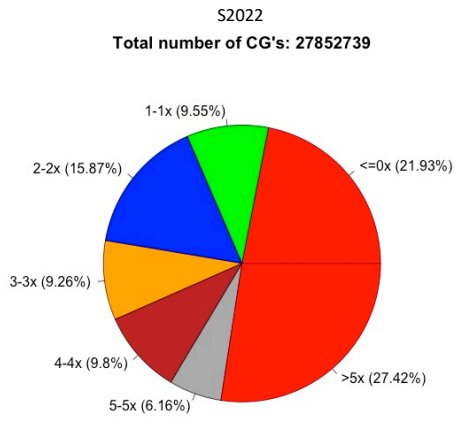

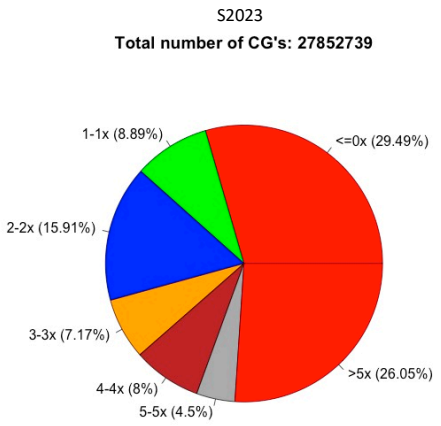

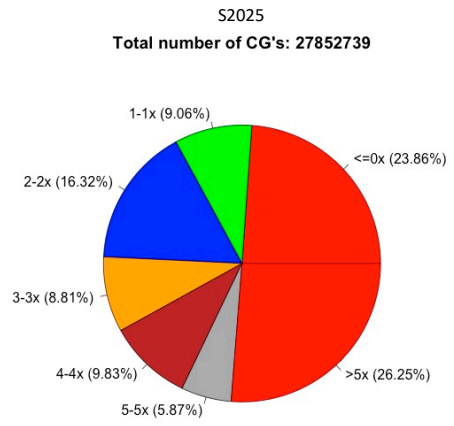

Supplementary Figure S5: Whole-genome CpG coverage for each sample. Genome-wide CpG coverage and depth depicted as the percentage and coverage level of the 28 million CpGs covered by the sequence reads. Reads are extended to length 180 bp (library mean length) and only one read mapped to same genomic location is kept (avoiding PCR duplicates).

Supplementary Figure S6

NH Staunstrup et al. 2017

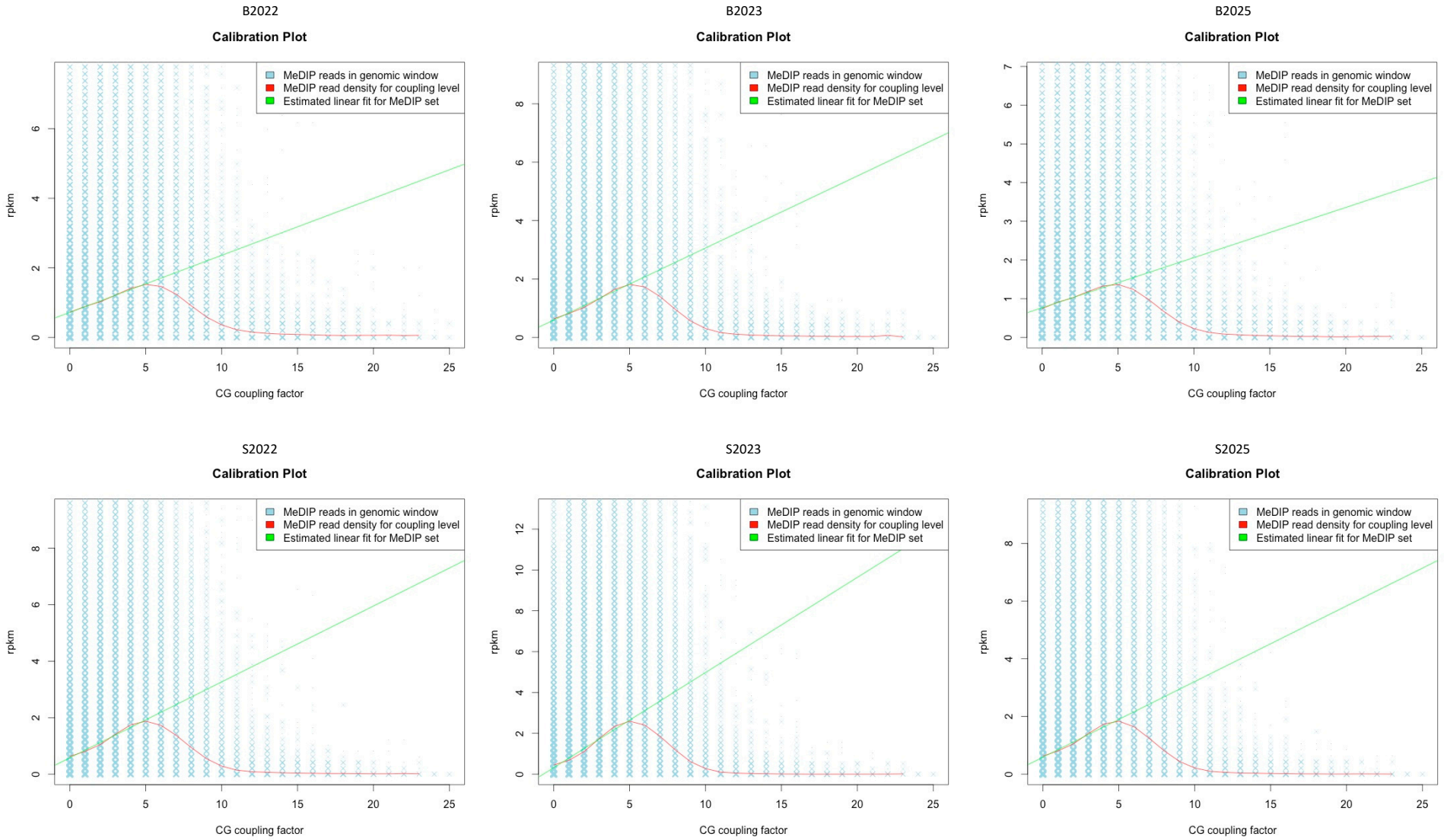

Supplementary Figure S6: CpG density dependent immunoprecipitation of DNA fragments. Calibration plot showing the CpG density dependent immunoprecipitation of DNA fragments in blood and saliva samples with normalization of number of reads per window. For illustrative purposes only chromosome 1 results are shown.

Supplementary Figure S7

A

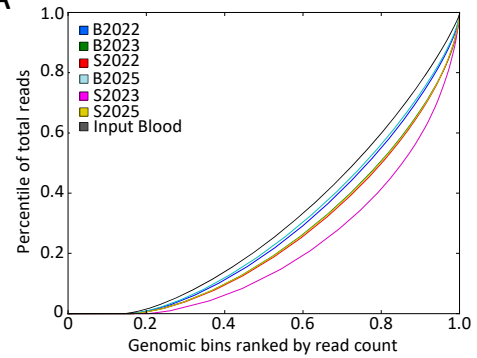

B

Sample ID	Enrichment score
B2022	1.14
B2023	1.25
B2025	1.10
S2022	1.30
S2023	1.48
S2025	1.29

Supplementary Figure S7: Enrichment of CpG. (**A**) Fingerprint plot depicting read count as a function of ranked genomic bins for saliva and blood samples and an input control (peripheral blood sample); (**B**) Enrichment score for CpG sites shown as the ratio of CpGs in MeDIP enriched DNA from saliva and blood samples compared to the reference genome.

Supplementary Figure S8

NH Staunstrup et al. 2017

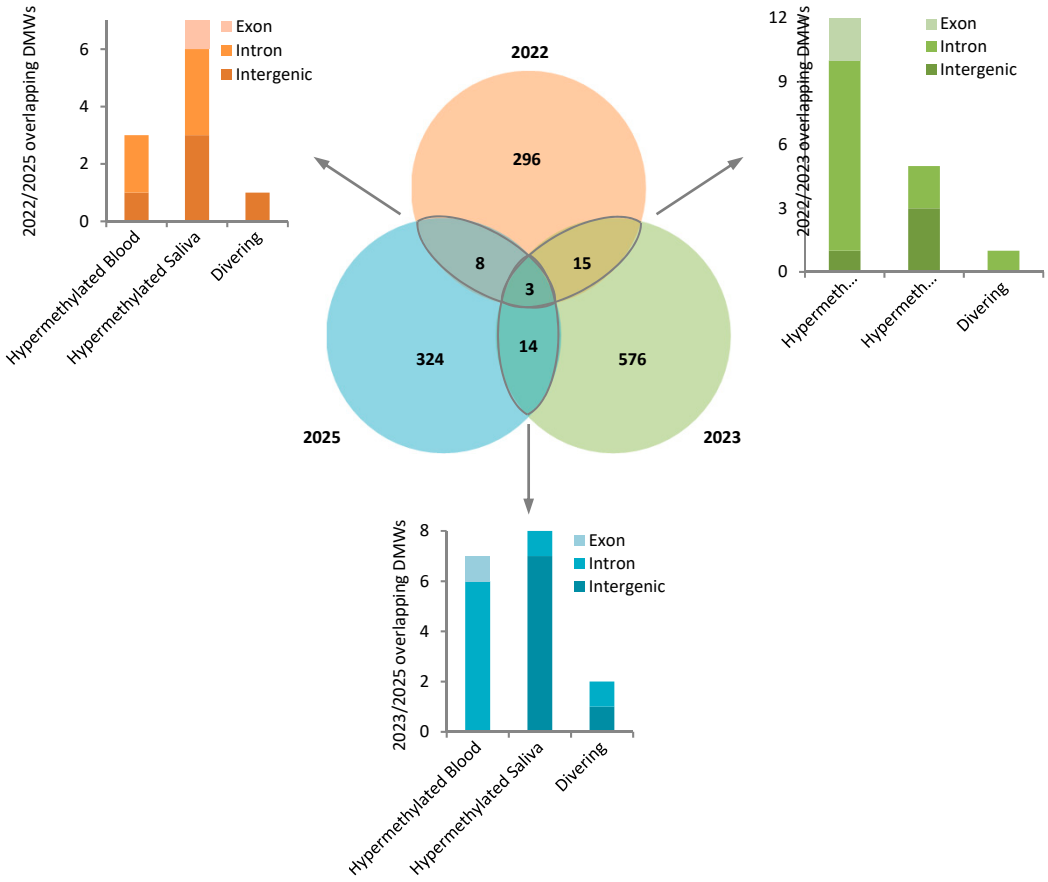

Supplementary Figure S8: Intra-individual DMWs. Venn diagram presenting the number of DMWs found in each intra-individual comparison and the overlap. Also included are bar charts of the pair-wise overlap of DMWs segregated by direction and genomic annotation.

Supplementary Figure S9

NH Staunstrup et al. 2017

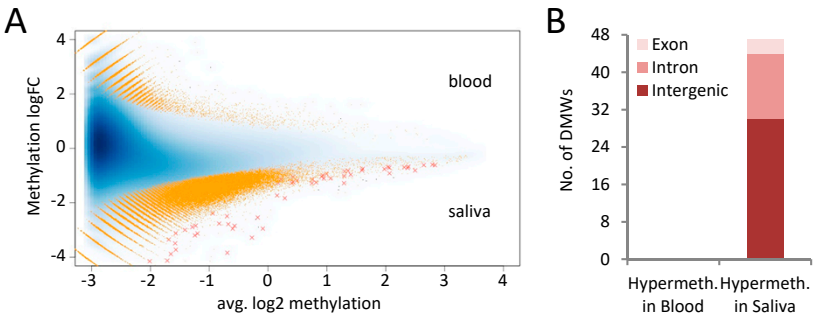

Supplementary Figure S9: Hypermethylated regions in saliva compared to blood. (**A**) MA plot depicting the average methylation level (*x*-axis) in the complete dataset against methylation difference (*y*-axis) between tissues. Yellow dots represent differentially methylated windows at $p < 0.001$ and red crosses significant DMWs with Bonferroni adjusted $p < 0.05$. A general tendency of a higher methylation rate in saliva is indicated from the cloud of orange dots with a downward trajectory, deviating from the mean; (**B**) Genomic annotation of DMWs within the three genomic features: intragenic (including pseudogenes), intronic, and exonic.

Supplementary Figure S10

NH Staunstrup et al. 2017

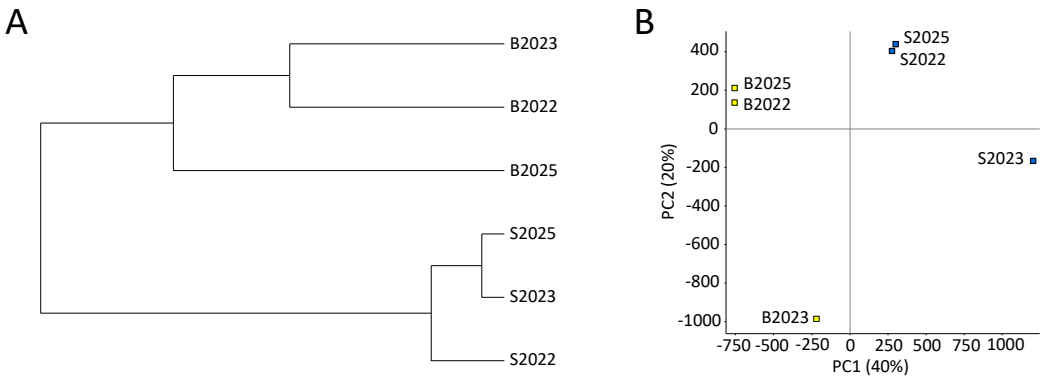

Supplementary Figure S10: Improved within-tissue clustering at downstream intragenic CGI shores. (**A**) Dendrogram of saliva and blood samples; (**B**) PCA plot of PC1 and PC2 using only sequencing reads overlapping downstream intragenic CGI shores.

Supplementary Figure S11

NH Staunstrup et al. 2017

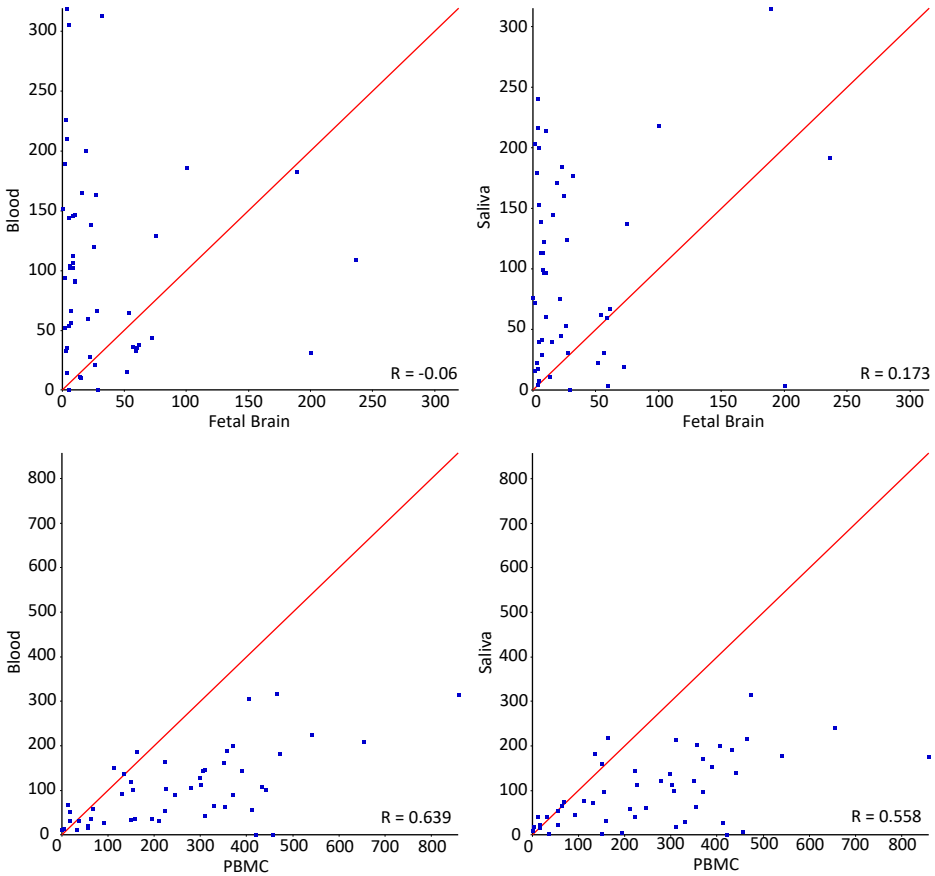

Supplementary Figure S11: Correlation was larger between related tissues compared to unrelated tissues. The correlation was based on 50 TS-DMRs.

Supplementary Table S1

DAVID (Default settings)	Term	Number of Genes in Input List	Fold Enrichment	P-value	BH Corrected P-value
UP_KEYWORDS	Alternative splicing	378	1.4	6.8E-21	2.5E-18
UP_KEYWORDS	Phosphoprotein	305	1.4	4.5E-16	8.0E-14
UP_SEQ_FEATURE	Splice variant	271	1.3	1.0E-09	1.7E-06
UP_KEYWORDS	Acetylation	136	1.5	1.2E-07	1.5E-05
GOTERM_CC_DIRECT	Cytoplasm	186	1.3	1.8E-05	8.2E-03

Supplementary Table S1: DAVID functional annotation. Employing default databases, terms passing Benjamini-Hochberg correction of the 577 genes featuring differently covered downstream intragenic CGI shores. UP; Uniprot.

Supplementary Table S2

DAVID (UP_TISSUE)	Term	Number of Genes in Input List	Fold Enrichment	P-value	BH Corrected P-value
UP_TISSUE	Brain	281	1.3	1.9E-07	3.7E-05
UP_TISSUE	Peripheral blood lymphocyte	5	5.8	1.0E-02	6.4E-01
UP_TISSUE	Epithelium	96	1.3	1.2E-02	5.4E-01
UP_TISSUE	Pancreatic Islet	4	7.0	1.8E-02	5.9E-01
UP_TISSUE	Reticulocyte	3	13.9	1.8E-02	5.1E-01
UP_TISSUE	Cajal-Retzius cell	13	2.1	2.5E-02	5.5E-01
UP_TISSUE	Kidney	56	1.3	2.8E-02	5.5E-01
UP_TISSUE	Primary B-cells	5	3.8	4.3E-02	6.6E-01
UP_TISSUE	Fetal brain cortex	13	1.8	6.6E-02	7.7E-01
UP_TISSUE	Cerebellum	27	1.4	6.6E-02	7.4E-01

Supplementary Table S2: DAVID functional annotation restricted to tissue expression. Using only Uniprot tissue (up_tissue) annotation database the 10 most significant terms applying the list of 577 genes featuring differently covered downstream intragenic CGI shores are displayed.